# Expanded View Figures

**Figure EV1. Characterization of OXPHOS super-assembly in zebrafish.**

A–C Split channels of BNGE of mouse (M) C57BL/6J (111), CD1(113), and zebrafish (ZF) muscle mitochondria shown in Fig 1A and B.

D, E Immunodetection of the indicated proteins after 2D BNGE/DDM electrophoresis of whole-body zebrafish mitochondria (representative of $n = 3$). Merged (D) and (E) split channels.

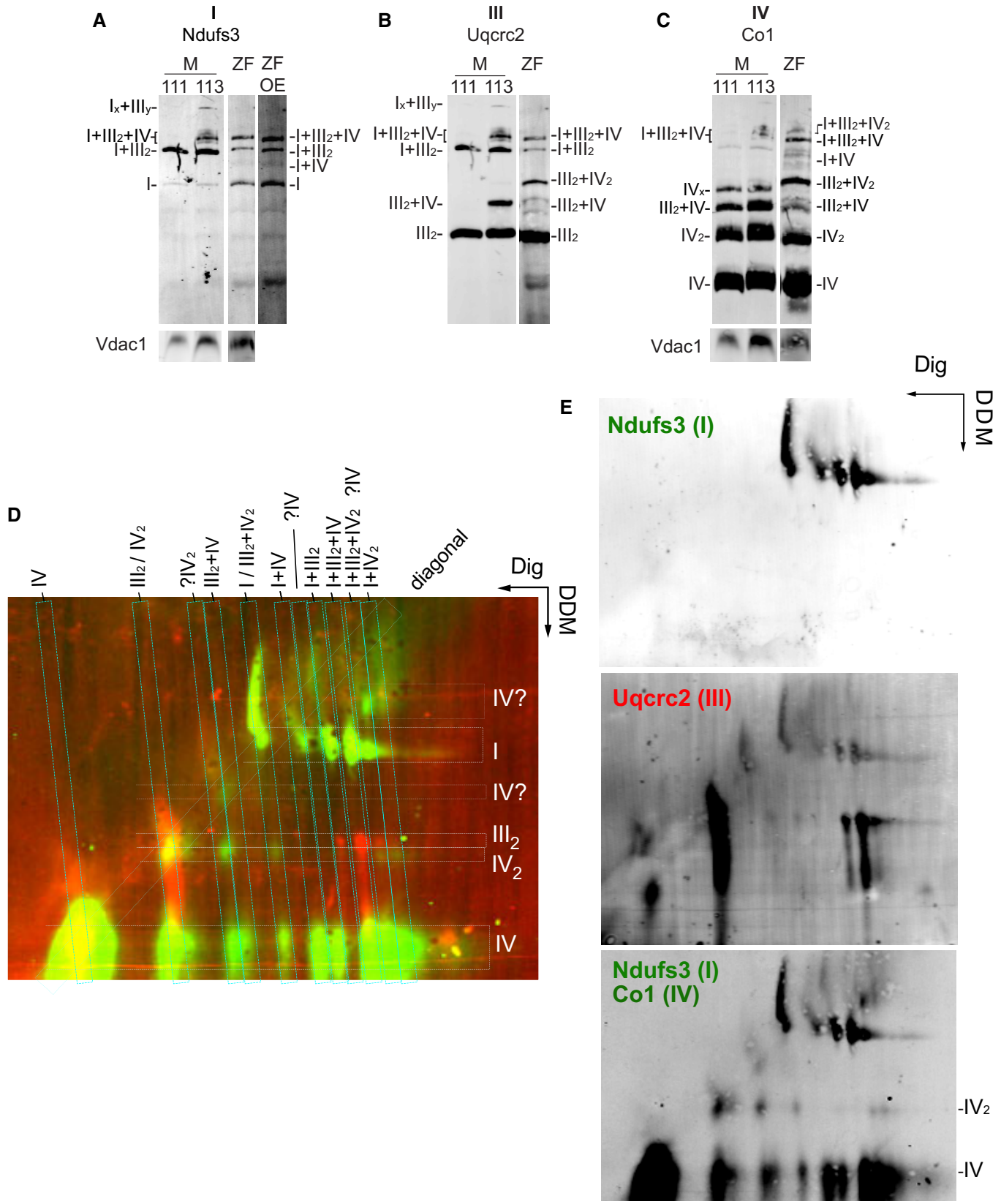


**Figure EV1.**

**Figure EV2. OXPHOS super-assembly in whole zebrafish and mouse liver in homeostasis and low-protein/low-fat diet.**

A–E BNGE of mouse (M) C57BL/6J (111) and CD1(113) liver mitochondria and zebrafish (ZF) whole-body mitochondria, digitonin-solubilized. (A–C) Immunodetection of the indicated proteins, (D) CI and (E) CIV in-gel activity (representative of two technical and three biological replicates).

F Immunodetection of the indicated proteins of digitonin-solubilized whole-body zebrafish mitochondria with different concentrations of digitonin.

G–I BNGE of zebrafish fed with low-protein/low-fat diet (LP/LF) and control diet (CD). (G) variation of BMI of fish after 6 weeks in LP/LF and CD (H) Representative images. (I) Representative BNGE of whole fish mitochondria of fish fed during 6 weeks in the indicated diet (experimental replicates $n = 2$ are composed by a pool of $n = 2$ biological replicates).

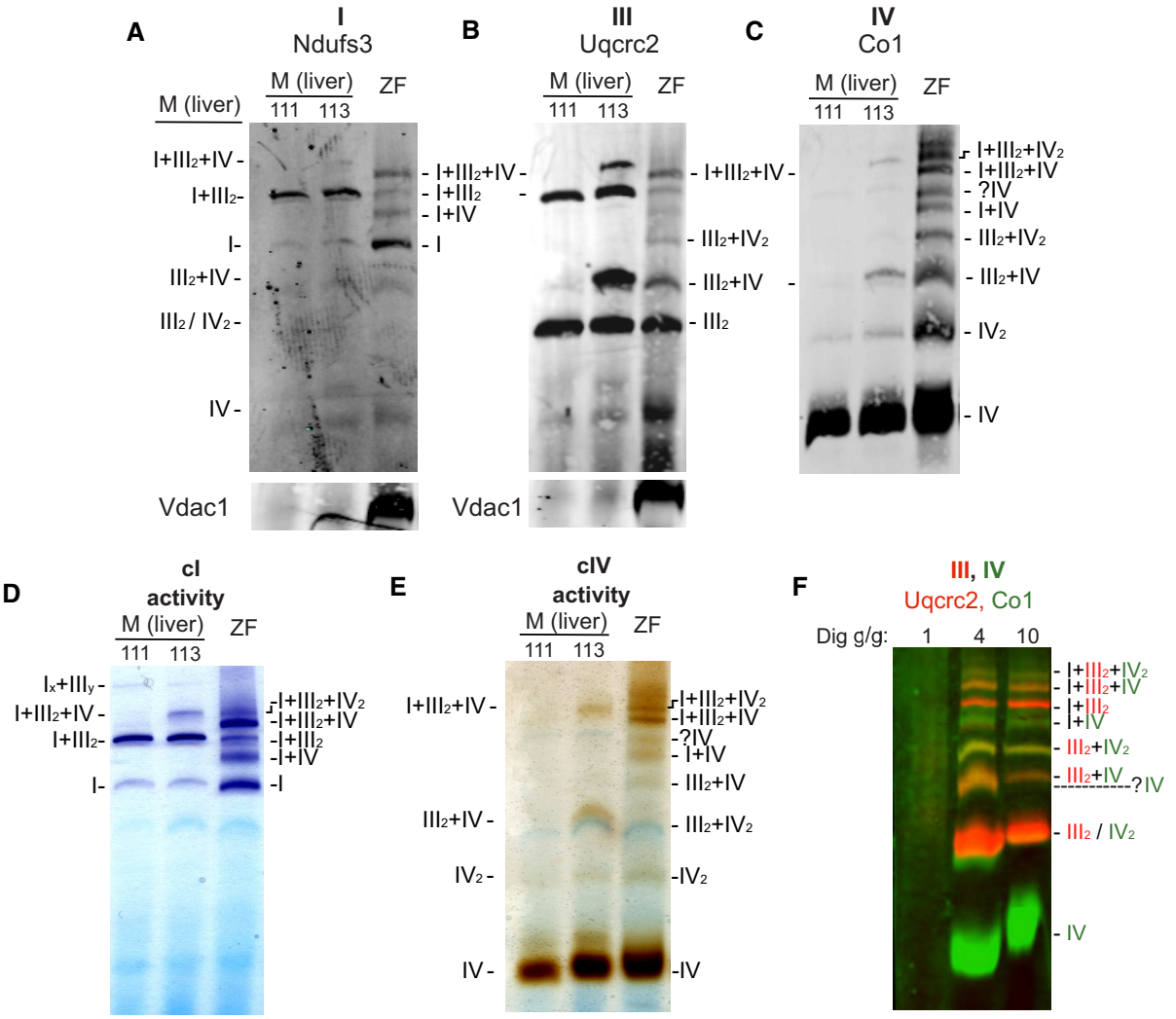


## LOW PROTEINS / LOW FAT DIET

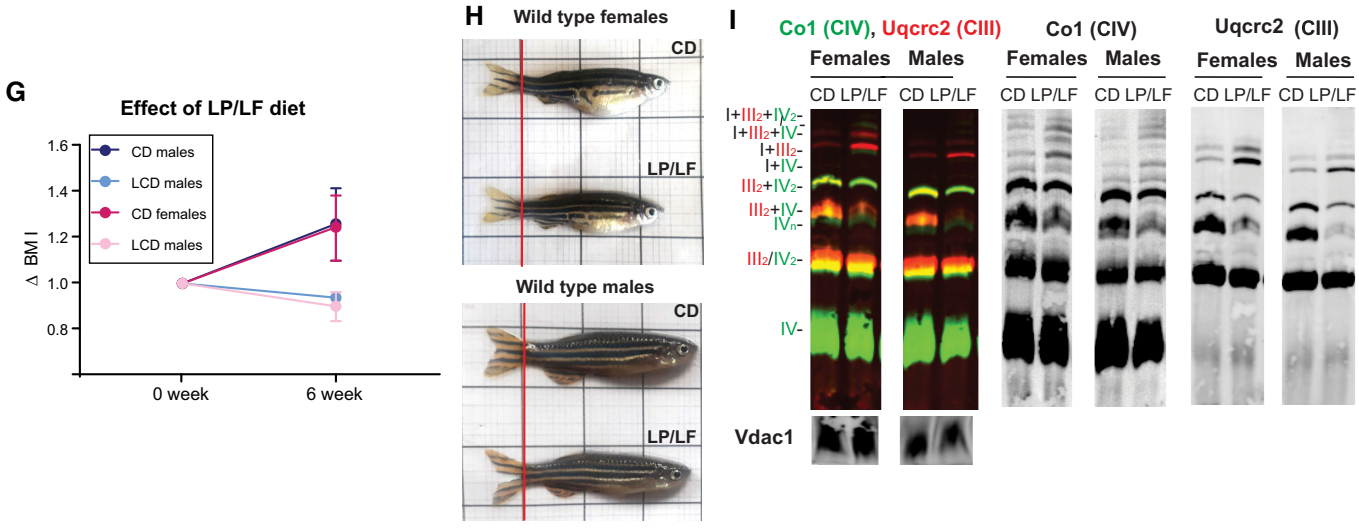


**Figure EV2.**

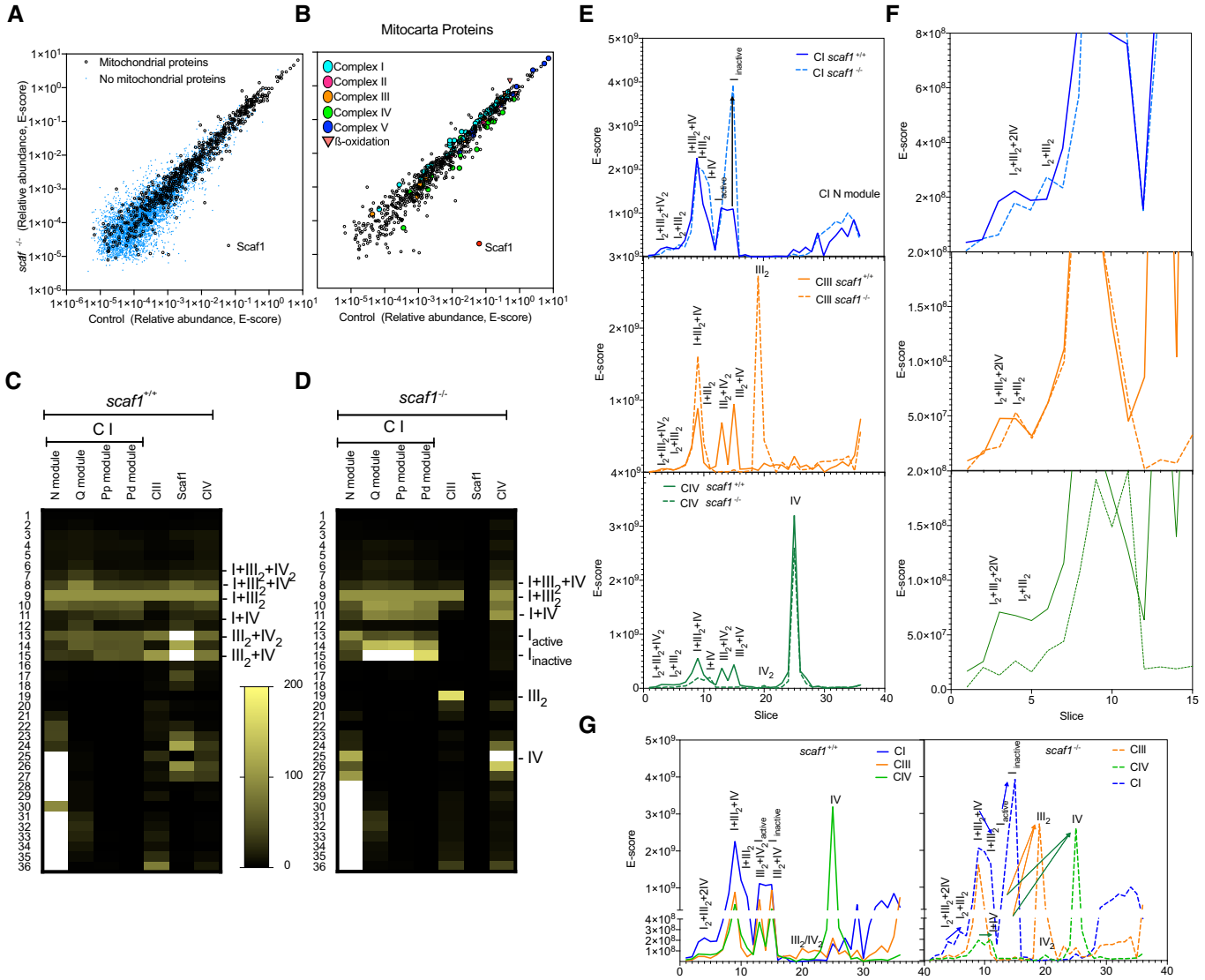


**Figure EV3. Analysis of mitochondrial complexes by Blue-DiS proteomics.**

A, B Correlation between the abundance of proteins (expressed as sum of *E*-scores of the corresponding peptides) detected in the analysis of *scaf1*$^{+/+}$ and *scaf1*$^{-/-}$ animals. Proteins were considered mitochondrial according to the classification in the mouse MitoCarta 2.0 database. Non-mitochondrial proteins include true non-mitochondrial proteins and potential mitochondrial proteins that failed to be identified as such. In (B), only the mitochondrial proteins are represented, indicating the proteins from the indicated groups.

C, D Heatmaps showing the summed absolute abundance of selected protein groups across BNGE gel slices. For a better comparison, absolute abundances were normalized using the values of slice 9 as a reference. Qualitative migration of the added *E*-score value for each indicated complex, subcomplex, or protein. For each line, data were normalized within a 100–0 range, with 100 being the value of slice 9. The color scale is established as a linear increase from black (being 0) to the green in slice 9 (being 100). Any value over 100 is white.

E–G Analysis of the quantitative differences between Blue-DiS profiles of *scaf1*$^{+/+}$ and *scaf1*$^{-/-}$ animals. Differences in quantity profiles of CI-, CIII-, and CIV-related complexes and SCs in (E) control and (F) *scaf1*$^{-/-}$ samples. The insets focus on the differences at very high molecular weights (slices 1–15). (G) Comparative analysis of quantitative profiles of complexes and SCs in control or *scaf1*$^{-/-}$ samples. Arrows indicate increase, decrease, or shifts of complexes observed between *scaf1*$^{-/-}$ and control samples.

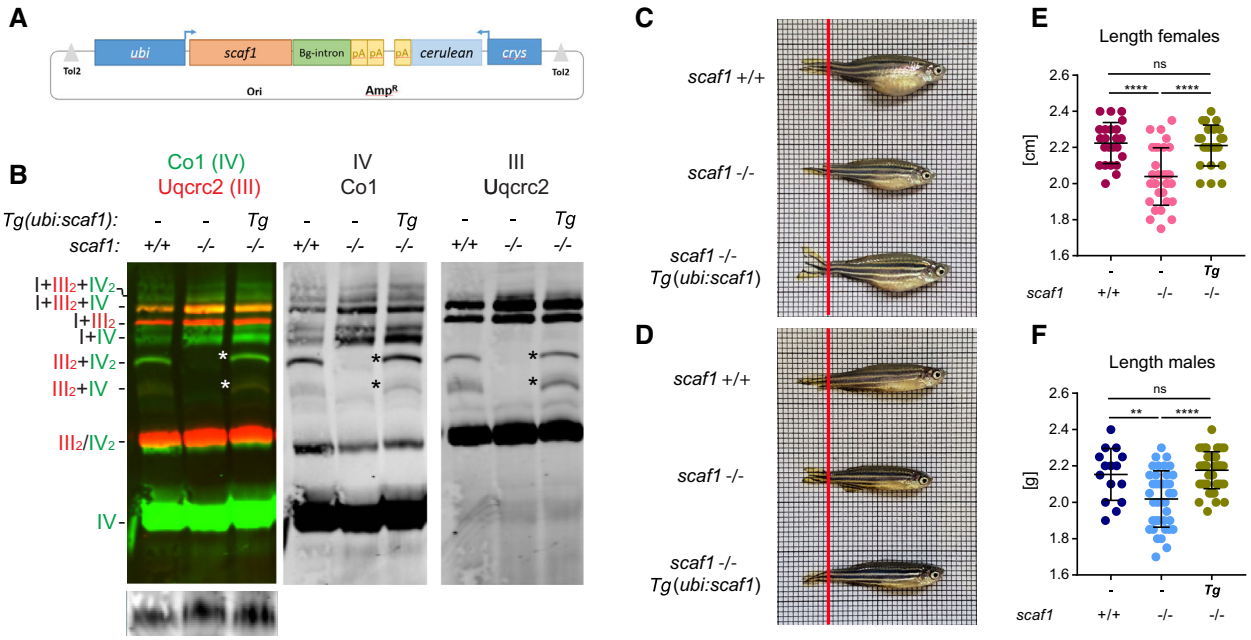


**Figure EV4. Transgenic expression of *scaf1* recovers CIII and CIV super-assembly and fish size of *scaf1*$^{-/-}$ fish.**

A Scheme of the transgenic construct *Tg*(*ubi:scaf1*). ubi, ubiquitin promoter. Bg-intron, beta-globin intron, pA, poly A, *crys*, crystalline promoter (used as selection marker).

B Immunodetection of the indicated proteins of BNGE from whole fish mitochondria *scaf1*$^{\Delta1/\Delta1}$ (−/−) expressing the transgenic construct *Tg*(*ubi:scaf1*) in heterozygosis, their *scaf1*$^{\Delta1/\Delta1}$ siblings with no transgenic expression, and *scaf1*$^{+/+}$ zebrafish (representative BNGE of $n = 5$). Asterisks mark bands' absence in *scaf1*$^{\Delta1/\Delta1}$ (−/−) recovered by the transgenic expression of *scaf1*.

C, D Representative images from *scaf1*$^{+/+}$, *scaf1*$^{\Delta1/\Delta1}$ (*scaf1*$^{-/-}$), and scaf1$^{-/-}$, Tg/− (C) female and (D) male zebrafish (3 mpf).

E, F Size of *scaf1*$^{+/+}$, *scaf1*$^{\Delta1/\Delta1}$ (*scaf1*$^{-/-}$), and scaf1$^{-/-,\ Tg/-}$ fish (E) length of females (*scaf1*$^{+/+}$ $n = 23$, *scaf1*$^{-/-}$ $n = 39$ and *scaf1*$^{-/-,\ Tg/-}$ $n = 25$); and (F) males (*scaf1*$^{+/+}$ $n = 15$, *scaf1*$^{-/-}$ $n = 31$ and scaf1$^{-/-,\ Tg/-}$ $n = 44$).

Data information: One-way ANOVA. ns $P > 0.05$, **$P < 0.01$, ****$P < 0.0001$. Data are represented as mean ± SD.

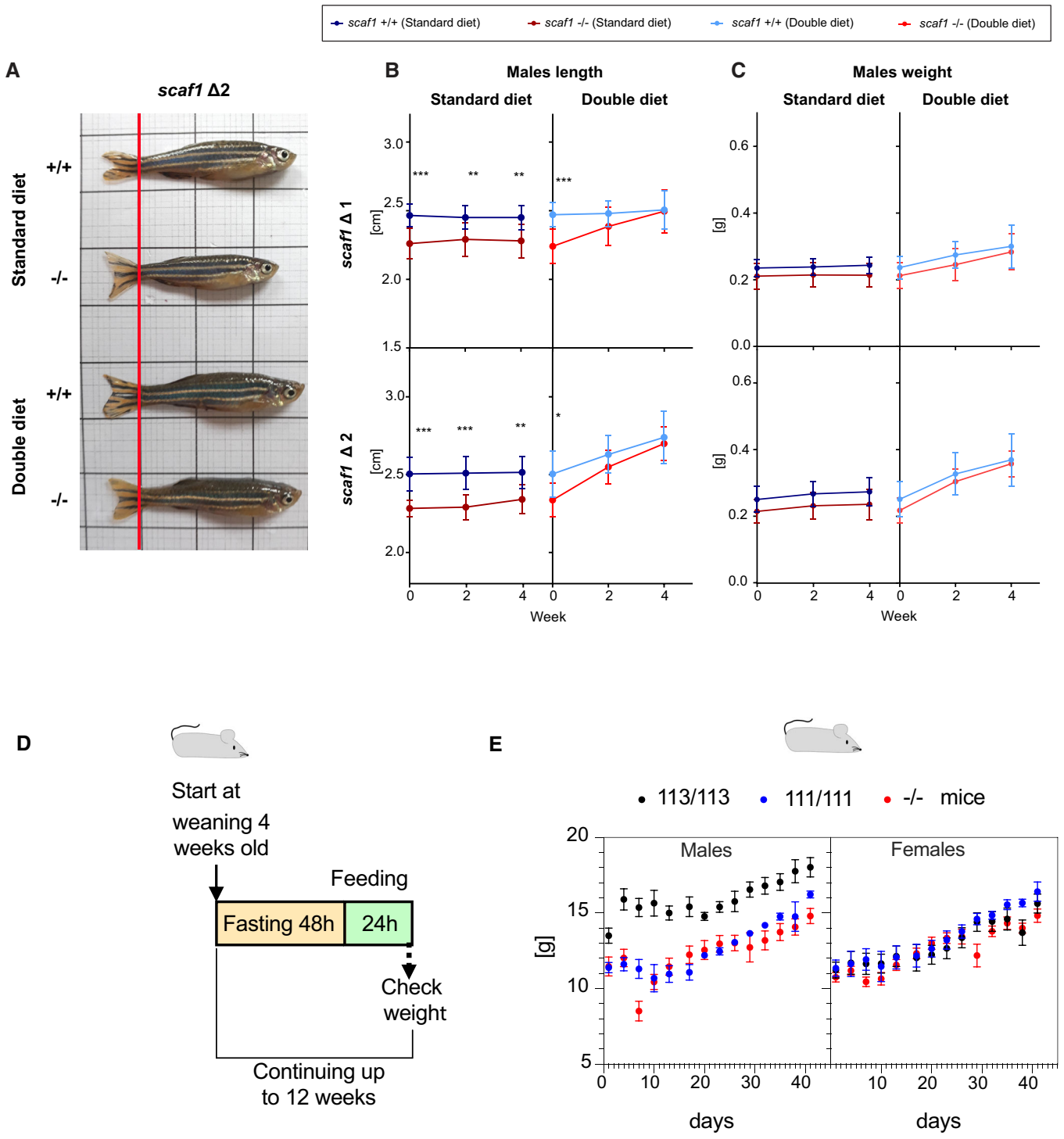


**Figure EV5. Diet-induced recovery of *scaf1*$^{-/-}$ phenotypes in males and diet effect in SCAF1-deficient mice.**

A Representative images of *scaf1*$^{-/-}$ and *scaf1*$^{+/+}$ males fed with the indicated diets.

B, C Size of males after the indicated diet. (B) Changes in length and (C) weight over time (Δ1 +/+ $n$ = 10, Δ1 −/− $n$ = 10, Δ2 +/+ $n$ = 10, Δ2 −/− $n$ = 7–8).

D, E Effect of SCAF1 loss of function on weight gain in mice after starvation. (D) Scheme of the food restriction experiment in mice. (E) Impact of food restriction in C57BL/6JOlaHsd mice with the functional version of SCAF1 113/113, with the spontaneous mutation in SCAF1 111/111 (natural C57BL/6JOlaHsd mice harbor a non-functional version of SCAF1) and in C57BL/6JOlaHsd mice without SCAF1 (SCAF1 KO, −/−). Males 111/111 $n$ = 3; males KO $n$ = 6; males 113/113 $n$ = 2; females 111/111 $n$ = 5; females KO $n$ = 8; females 113/113 $n$ = 5.

Data information: (B, C) Two-way ANOVA. Data are represented as mean ± SD. *$P$ < 0.05, **$P$ < 0.01, ***$P$ < 0.001. (E) Data are represented as mean ± SEM.